

Light-Field Approximation Using Basic Display Layer Primitives

Nicola Ranieri
ETH Zürich

Simon Heinzle
Disney Research
Zurich

Peter Barnum
Disney Research
Zurich

Wojciech Matusik
CSAIL, MIT

Markus Gross
Disney Research
ETH Zürich

Abstract

A new concept using different display layer primitives for light field approximation is presented. For each primitive, a mathematical notation for the light transport operator is defined. Based on that, a decomposition algorithm rendering a light field into a multi-layered plenoptic display is described and verified by a physical prototype.

Author Keywords

display; light field; multi-layered; plenoptic function; display primitives; light field decomposition; light transport.

1. Introduction

Glasses-free 3D displays have experienced a major renaissance in the past few years. In general, these displays can be divided into two main categories: parallax-based displays and volumetric displays. Parallax-based approaches such as integral imaging [11] and parallax barriers [8] redirect spatially varying pixels onto different viewing directions. These approaches trade off spatial resolution in favor of angular resolution, which directly relates to the depth range that can be displayed without aliasing [4]. Though being capable of view dependent effects and proper occlusions, these devices often exhibit low spatial or angular resolution and lack correct accommodation cues. Volumetric displays [[5],[9],[13]], on the other hand, physically deploy light-emitting voxels in 3D space and provide a direct and natural approximation of the input scene. They provide correct accommodation cues but are, with few exceptions, not capable of providing proper occlusions or view dependent effects. A comprehensive overview of volumetric displays is given in [7].

As alternative, multi-layered displays [[1],[2],[12],[14],[15]] have been suggested to provide natural ways to show 3D scenes at nearly correct accommodation cues with increased display bandwidth and hence higher angular and spatial resolution. In essence, these displays combine parallax and volumetric displays and draw benefits from both. In our work, we generalize these concepts to multi-layered plenoptic displays by defining basic display layer primitives, consisting of emissive and modulating layers. We provide a mathematical framework to describe light transport through any combination of such layers. Based on this framework, we then provide a method to distribute an input light field according to a given display configuration. Furthermore, a quantitative error analysis for different layer configurations is provided. Finally, we present a

physical prototype, capable of rendering volumetric content with view dependent effects, proper occlusions and better accommodation cues.

In the rest of the paper, we will first present the mathematical framework for our display model. Then, we introduce our approach to distribute an input light field of a 3D scene to multiple emissive and modulating layers. Finally, we show a quantitative analysis and our display prototype.

2. Mathematical Framework

Our model assumes co-planar display layers which are aligned with the xy plane. Each of the layers can be either emitting or modulating, performing a certain operation on the overall light transport.

Our model is using a similar notation and concepts as presented by Durand et al.[6]. In general, the light field ℓ describes the radiance of light rays passing through points (x,y) and (u,v) at distance z from the xy plane, and is denoted as $\ell(x,y,z,u,v)$. For simplicity, we will only consider light rays traveling along the positive z direction, as our displays will only be viewed from the front.

Light Transport in Free Space: The basic light transport is illustrated in Figure 2 (middle). A ray starting at position (x,y,z) passing through (u,v) traverses in free space to

$$x' = x + \Delta z \cdot u, y' = y + \Delta z \cdot v$$

As the ray moves in depth, its position will change to $(x',y',z+\Delta z)$ while keeping its original traveling direction (u,v) .

Display Layer Primitives: Many of the display layer types deployed in modern systems can be generalized to two categories. We describe both categories as basic display primitive and provide a mathematical notation for the light transport operator. Together with the notation of light transport in free space, more complex systems made of any combination of such display primitive layers can be described.

Emissive Layer: An emissive layer E acts like an array of point light sources, emitting constant spherical light. We use the notation $Ez(x,y)$ as the light portion at x and y on the plane at depth z , radiating into all directions (u,v) . The emissive layer adds light to an input light field ℓ_i , and yields the output light field ℓ_o , as illustrated in Figure 2 on the left:

$$\ell_o(x,y,z,u,v) = \ell_i(x,y,z,u,v) + Ez(x,y)$$



Figure 1: Illustration of the steps of our light field decomposition. (1) volumetric rendering, (2) view-independent and (3) view-dependent occlusion culling, (4) view-dependent rendering on parallax type layer. Photographs are taken from our multi-layered display prototype.

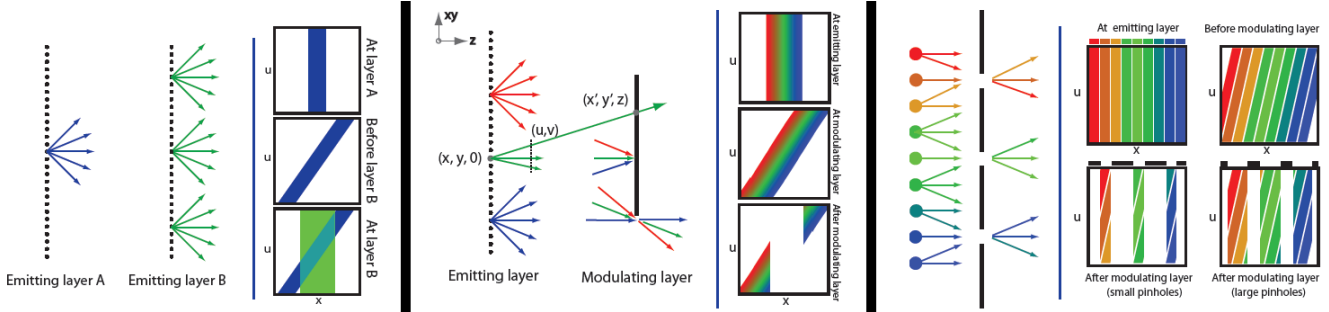


Figure 2: The three basic display layer primitives. Overlay of two emissive layers is shown on the left, impact of a modulating layer in the middle and the principle of a parallax barrier layer on the right.

Opaque emissive layers can be found in any 2D display consisting of e.g. a backlight with a modulating color LCD. However, to optically overlay them with other display layer primitives, transparent emitters are preferred. This can be implemented using the upcoming transparent OLED technology, by transparent anisotropic back-projection foils or, as in our prototype, polymer dispersed liquid crystal (PDLC) layers in combination with a projector.

Modulating Layer: A spatial modulating plane M will gradually attenuate all rays (u,v) passing through a certain pixel (x,y) . The modulating layer $Mz(x,y)$ is therefore represented as scalar between zero and one, and the output light field can be described as:

$$lo(x,y,z,u,v) = li(x,y,z,u,v) \cdot Mz(x,y)$$

The operation is shown in Figure 2 in the middle. Modulating layers can be implemented by (grayscale) liquid crystal displays, as the polarization rotation capability of twisted nematic liquid crystals can be used to block light when combined with two polarizers.

Parallax Barrier Layer: Parallax barrier displays are basically a combination of an emissive layer and a modulating layer with a special modulating pattern and small spacing Δz between the two layers. Therefore, the same light transport operators as for above layers are used. Since this pairing is fundamental, we define it as third basic primitive shown in Figure 2 on the right. The modulating layer is used to achieve ray separation by displaying a vertical slit, diagonal slit or pinhole pattern, while the emissive layer displays the different rays that pass through the slits/pinholes. As a consequence, an observer will see different rays from different directions. N pixels on the emitter plane can be partitioned into any number of spatial and angular samples (x,y,u,v) , such that $N > x \cdot y \cdot u \cdot v$. In practice, such displays trade a substantial reduction of spatial resolution for a relatively small amount of rays and apparent depth. The work of Levin et al. [10] provides a good background on this subject.

3. Light Field Decomposition

Based on the mathematical framework introduced in the previous section, we will describe an algorithm that approximates an input light field $li(x,y,z,u,v)$ as an output light field $lo(x,y,z,u,v)$ targeted for a given multi-layer plenoptic display, as illustrated in Figure 4. Our algorithm decomposes the input light field into a number of components. Each component is then displayed on one or multiple display primitives. In order to aid the decomposition process, we assume that for all rays (x,y,z,u,v) of the input light field we know the depth z of the

closest object, the view independent components (e.g. the diffuse part), and the view dependent components (e.g. the glossy/specular part).

In a first step, all diffuse components are assigned to their closest emissive layer, orthogonally projected onto them and rendered with high spatial resolution. This corresponds to naïve volumetric rendering and parts of the light field will be blended together as can be seen in Figure 1 on the left side. Parts of the light field not visible within the display field of view can be discarded completely, resulting in the second image in Figure 1.

In a second step, occlusions between layers are computed. Optimally, each emissive layer is preceded by a modulating layer to provide correct occlusions. However, as modulating LCD layers often absorb much light, a fewer number of modulating layers is desired. Hence, for each emissive pixel, occlusions for all emissive layers in front are detected, and the modulating layer closest to but behind the occluding layer is used for masking. The occlusion mask is retrieved by intersecting the ray from the emissive pixel to its occluding pixel with the chosen modulating layer. This step creates black borders (illustrated in the third image in Figure 1 or the bottom of Figure 8) since occlusions are detected conservatively over the whole viewing angle.

In a last step, these black borders are refilled and other view-dependent light field portions are added. Due to the planar mapping to the emissive layers, the holes cannot be filled naively. Our solution stretches the occluded residual to match the gap borders as illustrated on the left hand side of Figure 3, which corresponds to a scale in depth as shown on the right hand side. The same has to be considered for the glossy parts: They are mapped to the same plane as the view independent/diffuse part before being rendered. All components of this third step are rendered using the closest parallax barrier layer and have to be filtered accordingly using existing approaches [16]. A result of the complete algorithm is shown on the right of Figure 1.

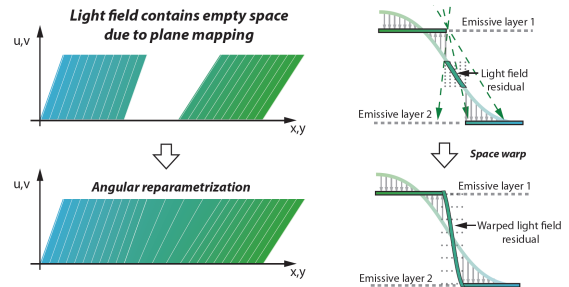


Figure 3: Adaptive hole filling between emissive layers.

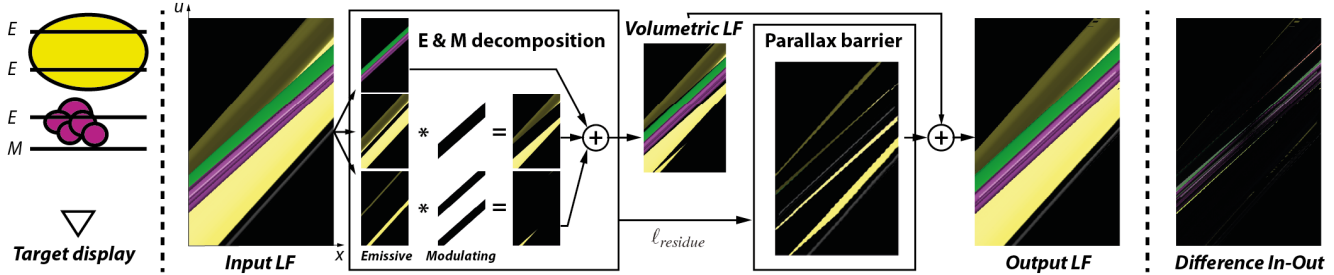


Figure 4: Illustration of the decomposition algorithm for a display layer configuration of one modulating layer followed by three emissive layers. View independent emissive elements are assigned, occlusions computed and the residue added using parallax barrier rendering.

4. Quantitative Analysis

To analyze the impact of number of layer primitives, we compare the resulting reprojection errors using our software simulation. We simulated two different scenes: a duck scene containing two objects at different depths with occlusion, and a bust scene depicting a continuous surface. Both scenes contain a small amount of specular highlights. The simulated results are compared to a perfect rendering, and the MSE between the simulated and perfect images are computed for a number of views in a field of view of 15°. The resulting error plots are shown in Figure 5.

In the left plot, the impact of an increasing number of emissive layers is depicted for three cases: In a first case, each emissive layer is preceded by a modulating layer, providing perfect occlusions for scene content in the back (red plots). In a second and third case, only one modulating layer is deployed front most and view dependent content is added by low resolution (green plots) or full resolution (blue plots) light field rendering. The error decreases fast when adding the first few layers, however, adding more than 4 layers does not reduce the error significantly.

In the right plot, the impact of an increasing number of modulating layers is assessed for a fix number of six (red plots), four (green plots) and three (blue plots) emissive layers. For this analysis, the modulating layers are placed after each emissive layer, starting from the front-most layer. An increasing number of modulating layers helps to reduce the error significantly. The plots furthermore show that increasing the number of emissive layers without increasing the number of modulating layers leads to significant high errors due to incorrect occlusions, perceived as black gaps as shown in Figure 8 on the bottom.

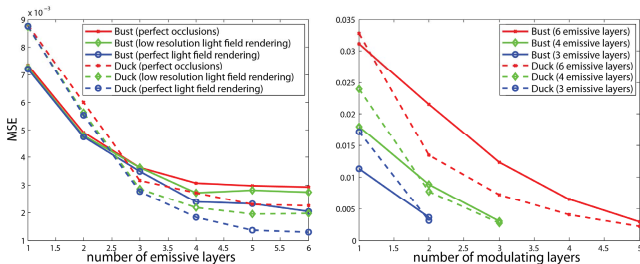


Figure 5: Quantitative error analysis using simulated results. Impact of an increasing number of emissive (left) as well as modulating layers (right) is evaluated.

5. Physical Prototype

We provide an example configuration in a physical prototype. It deploys three PDLC layers in combination with a projector to approximate the emissive layer primitive, and an LCD in the front as modulating layer. In each frame, one of the PDLC layers is opaque and diffuses incoming light while the others are transparent. This allows showing different images on different layers in time-multiplexed manner, similar to [13]. The PDLC layers are driven by the circuitry shown in Figure 1 which creates an alternating square wave function, preserving damages to the liquid crystal structures. The circuitry is synchronized with the v-sync signal of the projector such that the opaque layer is switched with each newly projected frame. As modulating layer, we employ an LCD with non-diffusing polarizing films. This layer is front most and used both to provide approximated occlusion as well as to render the light field portion of our decomposition algorithm.

The PDLC layers are spaced at 4mm, 10mm and 16mm from the front LCD. The projector has XGA resolution and a refresh rate of 60Hz, matching the refresh rate of the used PDLC layers. The front LCD renders 12 views in a 10° field of view when used as parallax barrier layer. The effective refresh rate of the display is 15Hz, since the front most emissive layer is used both for volumetric rendering as well as for parallax barrier rendering. The complete setup is shown in Figure 7.

Multi-layer plenoptic displays with homogeneous and well-aligned optical elements do not require calibration, since pixels are stacked directly behind each other in a one-to-one correspondence. However, in our setup we combine heterogeneous elements such as the projector and the LCD, which makes software calibration necessary. We propose a variant of the calibration scheme proposed in [1], and perform homography estimation based on photographs of projected checkerboard patterns.

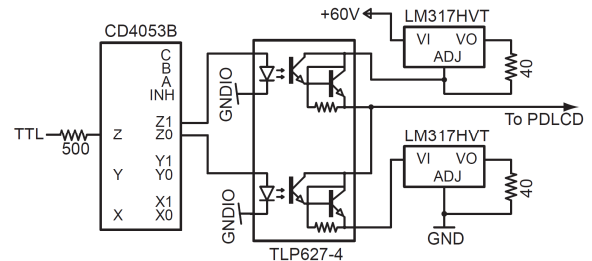


Figure 6: Circuitry used to create an alternating square wave function to drive the PDLC layers.

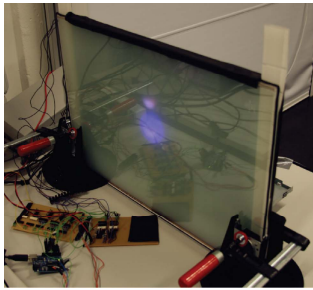


Figure 7: Our physical prototype consists of three emissive layers and a front most modulating layer.

6. Conclusion

We have introduced a general concept of multi-layer plenoptic displays. These display systems fuse multiple emissive and spatially modulating layers. First, we have presented a mathematical framework to analyze light transport for these displays. Second, we have described a rendering algorithm that takes as input a 3D scene and drives a given multi-planar system. Next, we have conducted an error analysis for multi-planar plenoptic displays. We then discussed practical issues of designing and building different display configurations. We demonstrate examples both in a simulation as well as on our physical prototype. Figure 1 shows all steps of our algorithm recorded on our multi-layered plenoptic display, each step decreasing the difference to the input light field. Figure 8 shows some of the simulated results that are used in our quantitative error analysis, supporting our insights about required number of layers. Though limitations imposed by current available hardware we believe our approach to suit a certain range of applications and will get more involved with upcoming technologies.

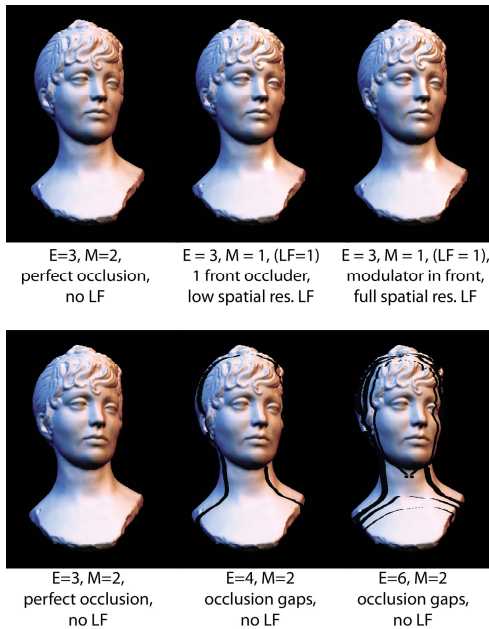


Figure 8: Simulated results used for the quantitative error analysis.

7. References

- [1] Annen, T., Matusik, W., Pfister, H., Seidel, H.-P., and Zwicker, M. "Distributed rendering for multiview parallax displays". In *Stereoscopic Displays and Applications, Proceedings of SPIE Vol. 6055* (2006).
- [2] Barnum, P.C., Narasimhan, S.g., and Kanade, T. "A multi-layered display with water drops". In *SIGGRAPH*, (2010).
- [3] Bell, G. P., Craig, R., Paxton, R., Wong, G., and Galbraith, D. "Beyond flat panels: Multi-layered displays with real depth". In *SID Symposium Digest of Technical Papers*, 39, 1, p. 352–355 (2008).
- [4] Chai, J.-X., Tong, X., Chan, S.-C., and Shum, H.-Y. "Plenoptic sampling". In *Proceedings of SIGGRAPH'00*, p. 307–318 (2000).
- [5] Coissart, O. S., Napoli, J., Hill, S. L., Dorval, R. K., and Favolora, G. E. "Occlusion-capable multiview volumetric three-dimensional display". *Applied Optics* 46, p. 1244–1250 (2007).
- [6] Durand, F., Holzschuch, N., Soler, C., Chan, E., and Sillion, F. X. "A frequency analysis of light transport". In *SIGGRAPH*, p. 1115–1126 (2005).
- [7] Favolora, G.E. "Volumetric 3D Displays and Application Infrastructure". In *Computer*, 38, 8, p. 37 – 44, (2005).
- [8] Ives, F. "Parallax stereogram and process for making same". US Patent No. 725,567, (1903).
- [9] Jones, A., McDowall, I., Yamada, H., Bolas, M., and Debevec, P. "Rendering for an interactive 360 light field display". *ACM Transactions on Graphics* 26, 3, (2007).
- [10] Levin, A., and Durand, F. "Linear view synthesis using a dimensionality gap light field prior". In *CVPR*, p. 1831–1838 (2010).
- [11] Lippmann, G.M. "La photographie integrale". *Comptes-Rendus* 146, p. 446-451 (1908).
- [12] Ranieri, R., Heinzle, S., Smithwick, Q., Reetz, D., Smoot, L.S., Matusik, W., and Gross, M. "Multi-layered automultiscopic displays". *Computer Graphics Forum* 31, 7, p. 2135–2143 (2012)
- [13] Sullivan, A. "DepthCube solid-state 3D volumetric display". In *SPIE Stereoscopic Displays and Virtual Reality Systems*, vol. 5291, p. 279–284 (2004).
- [14] Tamura, S., and Tanaka K. "Multilayer 3-D display by multidirectional beam splitter". *Applied Optics* 21, p. 3659–3663 (1982).
- [15] Wetzstein, G., Lanman, D., Hirsch, M., and Raskar, R. "Tensor Displays: Compressive Light Field Synthesis using Multilayer Displays with Directional Backlighting". *ACM Transactions on Graphics* 31, 4, (2012).
- [16] Zwicker, M., Matusik, W., Durand, F., and Pfister, H. "Antialiasing for automultiscopic 3D displays". In *Eurographics Symposium on Rendering* (2006).